

A Comparison of Ultraviolet and Visible Raman Spectra of Supported Metal Oxide Catalysts

Yek Tann Chua,[†] Peter C. Stair,^{*,†} and Israel E. Wachs^{*,‡}

Department of Chemistry, Center for Catalysis and Surface Science and Institute of Environmental Catalysis, Northwestern University, Evanston, Illinois 60208, and Zettlemoyer Center for Surface Studies and Department of Chemical Engineering, Lehigh University, Bethlehem, Pennsylvania 18015

Received: April 11, 2001

The recent emergence of ultraviolet-wavelength-excited Raman spectroscopy as a tool for catalyst characterization has motivated the question of how UV Raman spectra compare to visible-wavelength-excited Raman spectra on the same catalyst system. Measurements of Raman spectra from five supported metal oxide systems (Al_2O_3 -supported Cr_2O_3 , V_2O_5 , and MoO_3 as well as TiO_2 -supported MoO_3 and Re_2O_7), using visible (514.5 nm) and ultraviolet (244 nm) wavelength excitation have been compared to determine the similarities and differences in Raman spectra produced at the two wavelengths. The samples were in the form of self-supporting disks. Spectra from the oxides, both hydrated as a result of contact with ambient air and dehydrated as a result of calcination or laser-induced heating, were recorded. A combination of sample spinning and translation to produce a spiral pattern of laser beam exposure to the catalyst disk was found to be most effective in minimizing dehydration caused by laser-induced heating. Strong absorption by the samples in the ultraviolet significantly reduced the number of scatterers contributing to the Raman spectrum while producing only modest increases in the Raman scattering cross section due to resonance enhancement. The result was much lower signal levels with ultraviolet excitation compared to visible wavelength excited spectra. The absence of strong resonance enhancement effects in the ultraviolet also resulted in Raman spectra that were remarkably similar in terms of the vibrational bands observed, their Raman shift, and their pattern of intensities. Generally, the UV Raman spectra appear to be more sensitive to the out-of-plane bending and symmetric stretching vibrations of bridging oxygen species (M–O–M), whereas the visible Raman spectra are more sensitive to terminal oxygen vibrations (M=O). These differences suggest that a more complete characterization of the supported metal oxide species can be obtained by Raman measurements at several excitation wavelengths. Subtle differences in the spectra due to the extent of dehydration were also evident. These results indicate both that the Raman spectra are very sensitive to the nature of the supported metal oxide species and their environments, which requires that substantial care must be taken in the method of sample treatment during the measurements to obtain meaningful spectra.

Introduction

Supported metal oxide catalysts have wide applications in the chemical and petroleum industries.¹ Complete understanding of the catalytic properties of these metal oxides requires the determination of the structure–activity relationship of these materials. Vibrational spectroscopy has become a very powerful tool for characterizing the molecular structures of these supported metal oxides. Infrared spectroscopy has been used to study the interactions of the surface metal oxide species with the surface hydroxyls of the support.² It can also be used to measure the distribution of surface Brønsted and Lewis acid sites by adsorption of pyridine.³ The number of surface sites on these catalysts can also be estimated by measuring the amount of chemisorbed CO_2 .⁴ IR can also be used to detect the terminal metal–oxygen stretches (M=O) on supported metal oxides.⁵

Surface metal oxide species typically vibrate in the 100–1100 cm^{-1} region. Common oxide supports, such as γ -alumina and amorphous silica, absorb strongly below approximately 1000

cm^{-1} .⁶ Consequently, the IR bands of the surface metal oxide species are usually masked by the strong IR bands of the oxide support. In contrast, the Raman bands of these oxide supports are weak or Raman inactive in the same region.⁶ Because of this, Raman spectroscopy is preferred over IR spectroscopy for measuring the vibrational spectra of supported metal oxides. Since the Raman spectrum of each molecular structure is unique, Raman spectroscopy can discriminate between different molecular structures of the supported metal oxides. In the past 25 years numerous successful experiments, pertaining to the structural elucidation of the supported metal oxide species under ambient and in situ conditions, have been performed.^{6–9} More recently, success has also been achieved when Raman spectroscopy was used to conduct experiments under reaction conditions.^{10–12}

Occasionally sample fluorescence can mask the Raman spectrum of catalytic materials when using excitation by visible wavelengths. This phenomenon may be caused by the presence of carbon impurities or deposits, which are inevitably produced during some chemical reactions.¹³ It may also be due to traces of highly fluorescent transition metal ions¹³ or the presence of certain hydroxyl groups.¹⁴ Laser excitation in the near-IR¹⁵ or

* Authors to whom correspondence should be addressed.

[†] Northwestern University.

[‡] Lehigh University.

UV¹⁶ has been used to avoid fluorescence. UV excitation offers certain advantages over IR excitation. The frequency dependence in normal Raman scattering ensures that a Raman peak will be more intense under UV excitation than under IR irradiation. For chemical species that absorb UV photons, the resonance Raman effect may enhance the peak intensity further. In the past few years, UV Raman spectroscopy has been successfully employed to study various catalytic materials such as zeolites (fresh or heavily coked) or sulfated zirconia (fresh or heavily coked), under either ambient or reaction conditions.^{17–23} Fluorescence, in all cases, was completely avoided.

In the present paper, UV and visible Raman spectroscopy were employed to study the molecular structures of supported metal oxide species. The main objective of this work is to compare the Raman spectra taken under UV and visible radiation. We will also discuss possible scenarios where it would be more advantageous to use UV excitation than visible irradiation and vice versa for recording Raman spectra of supported metal oxide catalysts.

Experimental Section

A. Sample Preparation. The supported metal oxides were prepared at Lehigh University. They were prepared by incipient wetness impregnation using the appropriate precursors: chromium(III) nitrate for surface chromium oxides, vanadium triethoxide oxide or vanadium triisopropoxide oxide for surface vanadium oxide, ammonium heptamolybdate for surface molybdenum oxides, and perhenic acid for surface rhenium oxides. The impregnated samples were subsequently dried at room temperature, dried at 110–120 °C, and then calcined at high temperatures. The temperature of calcination depended on the specific metal oxides. Details of the preparations for each catalyst can be found in previous publications.^{24–28}

B. Raman Spectra. The UV Raman spectra of the supported metal oxides were measured using the UV Raman instrument built at Northwestern University. The excitation source was the 244 nm line from a Lexel 95 SHG (Second Harmonic Generation) laser equipped with an intracavity nonlinear crystal, BBO (Beta Barium Borate: BaB₂O₄) that frequency doubled visible radiation into mid-ultraviolet. The scattered photons were collected by an ellipsoidal mirror and focused into a Spex Triplemate (model 1877) triple monochromator. The photons were detected by an imaging photomultiplier tube (ITT, model F4146). The signal from the detector was subsequently analyzed by a position computer (Surface Science Laboratories, model 240) and presented in the form of a spectrum with the PCA3 program from Oxford Instrument Inc.. All UV Raman spectra were recorded under ambient conditions on samples in the form of 1.5 cm diameter, self-supporting disks. The UV Raman spectra were recorded from samples under three sets of conditions: (1) *Stationary* conditions where the laser beam was focused to a single spot on the face of the sample. These samples are designated as *dehydrated* since laser-induced heating produced partial dehydration of the sample within the laser beam. (2) *Spinning* conditions (~2000 rpm) where the laser beam was focused to a spot off the spinning axis. These samples are designated as *hydrated* since dehydration due to laser-induced heating is reduced. (3) *Spiral* conditions where the spinning sample was translated manually so that the laser beam moved from the center toward the edge of the disk. These samples are designated as *hydrated* since dehydration due to laser-induced heating was minimized. The spinning method was very effective in reducing dehydration due to local heating by the laser beam. Depending on the signal strength of each sample,

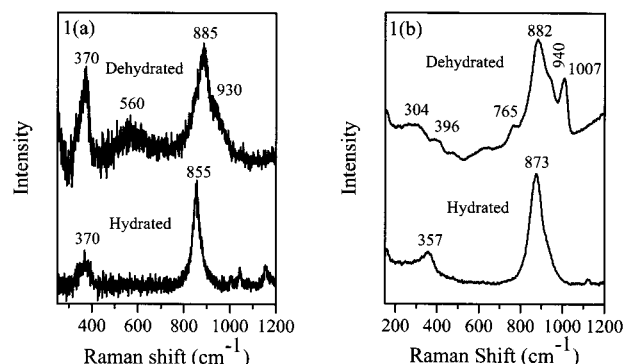


Figure 1. (a) UV Raman spectra of hydrated and dehydrated 0.5% CrO₃/Al₂O₃. (b) Visible Raman spectra of hydrated and dehydrated 0.5% CrO₃/Al₂O₃.

the laser power used was 5–20 mW. For alumina-supported metal oxides, the collection time for a UV Raman spectrum is from 1800 to 6000 s. For titania-supported samples, the Raman signals are relatively weaker and the collection time ranges from 10 800 to 51 600 s. A 2400 g/mm grating was used in second order to disperse the UV Raman spectra. Typical resolution achieved was 10–12 cm⁻¹. Details of the instrument have been previously published.²¹

The visible Raman spectra of supported metal oxides were measured at Lehigh University. The excitation source was the 514.5 nm line from an argon ion laser (Spectra Physics, model 171) delivering 10–20 mW of laser power at the sample. Each Raman spectrum was recorded in 900 s, significantly shorter collection than for the UV Raman spectra. The scattered radiation was directed into a Spex triplemate spectrometer (model 1877) coupled to a Princeton Applied Research OMA III optical multichannel analyzer (model 1463) equipped with an intensified photodiode array detector. The visible Raman spectra were collected and recorded using an OMA III (PAR) directed computer and software. Typical resolution was ~2 cm⁻¹. The Raman spectra of *dehydrated* and *hydrated* samples were recorded with stationary (under in situ conditions after dehydration at 450 °C) and spinning disks (under ambient conditions) (~2000 rpm), respectively.

The UV–visible diffuse reflectance spectra of the supported metal oxides were measured under ambient conditions using a Cary 1-E spectrophotometer from Varian Inc.

Results and Discussion

A. Alumina-Supported Metal Oxides. γ -Alumina is Raman inactive in the 100–1200 cm⁻¹ region.⁶ All Raman peaks are assigned to surface metal oxide vibrations unless stated otherwise.

1a. 0.5% CrO₃/Al₂O₃ (~4% monolayer). The UV and visible Raman spectra of 0.5% CrO₃/Al₂O₃ are presented in Figure 1, parts a and b, respectively. The UV Raman spectrum of the hydrated sample was measured using spiral conditions. The Raman bands at ~370 and 855 cm⁻¹ correspond to the bending modes and symmetric stretch of the hydrated CrO₄²⁻ species. The Raman bands of the bending modes of the aqueous CrO₄²⁻ ion appear at 348 and 371 cm⁻¹ while the symmetric stretch is at 846 cm⁻¹.²⁹ The shift of the symmetric stretch from 846 to 855 cm⁻¹ suggests that the sample is partially dehydrated. Due to the loss of some water molecules, the surface CrO₄²⁻ species interact weakly with the alumina support. This interaction distorts the chromate ion structure from its ideal T_d symmetry, and the distortion is manifested as a small shift of the Raman band to higher wavenumbers. The small bands at ~1050 cm⁻¹

and $\sim 1150\text{ cm}^{-1}$ are attributed to trace amounts of NO_3^- and CO_3^{2-} ions. The former species is retained in the sample following preparation while the latter originates from adsorption of ambient CO_2 .

When purely spinning (not spiral) conditions were used, a light brown ring formed where the UV laser beam irradiated the sample. Dark brown, polymeric species are known to form as a result of sample dehydration.³⁰ (0.5% $\text{CrO}_3/\text{Al}_2\text{O}_3$ is light yellow). The light brown ring suggests that the sample has undergone partial dehydration. Under spiral conditions, the products from laser-induced dehydration were spread over the whole surface of the sample disk instead of concentrated in a circle. In addition, the sample remained essentially yellow in color after the UV Raman measurement, and the small shift of $\sim 9\text{ cm}^{-1}$ suggests that the sample has retained most of its water of hydration.

The visible Raman spectrum of the hydrated supported chromium oxide was obtained under spinning conditions (Figure 1b), and the spectrum is similar to its UV counterpart in terms of the number of Raman bands and relative band intensities. The bending modes of the hydrated CrO_4^{2-} species appear at 355 cm^{-1} . The symmetric stretch of the hydrated CrO_4^{2-} species has shifted to higher wavenumbers. The shift from 846 cm^{-1} to 873 cm^{-1} suggests that the sample measured with visible excitation is more dehydrated than the one measured with UV excitation. These Raman measurements also indicate that the spiral condition is more effective in reducing the influence of local sample heating on the Raman spectrum than pure spinning.

The UV and visible Raman spectra of the dehydrated samples suggest the presence of a new surface metal oxide species. The appearance of bands at $\sim 560\text{ cm}^{-1}$ (symmetric stretch of bridging Cr–O–Cr groups) and $\sim 930\text{ cm}^{-1}$ (symmetric stretch of terminal CrO_2 /asymmetric stretch of terminal CrO_3 group) along with the upward shift of the CrO_3 symmetric stretch to 885 cm^{-1} suggest the existence of polymeric species by comparison to spectra of the aqueous chromate ion dimers, trimers, and tetramers.^{29,30}

The visible Raman spectrum of the dehydrated sample was recorded using a stationary sample under controlled atmosphere following calcination. The spectrum also suggests the existence of a polymeric species. The Raman bands at $304/396\text{ cm}^{-1}$, $\sim 765\text{ cm}^{-1}$, 882 cm^{-1} , $\sim 940\text{ cm}^{-1}$ and 1007 cm^{-1} correspond to the bending modes of CrO_3 and CrO_2 , asymmetric stretch of Cr–O–Cr, symmetric stretch of CrO_2 , symmetric stretch of CrO_2 and asymmetric stretch of CrO_3 (terminal) and asymmetric stretch of CrO_2 groups, respectively.

For the dehydrated sample, the 1007 cm^{-1} and $\sim 765\text{ cm}^{-1}$ bands are not detected in the UV Raman spectrum. On the other hand, the $\sim 370\text{ cm}^{-1}$ and $\sim 560\text{ cm}^{-1}$ bands are relatively more intense under UV excitation. These relative peak intensity variations may be due to residual hydration and to different extents of resonance enhancement for different Raman bands under UV excitation.

For the same vibrational mode, the corresponding band may not appear at the same Raman shift in the visible and UV excited spectra. For example, the Raman bands due to CrO_3 and CrO_2 bending vibrations in the polymeric species of dehydrated samples do not appear at the same Raman shift in the visible and UV excited spectra. A plausible explanation is the different degrees of dehydration of the samples used for measuring these spectra. As shown in the visible and UV Raman spectra of hydrated 0.5% $\text{CrO}_3/\text{Al}_2\text{O}_3$, the Raman band position of the CrO_4^{2-} symmetric stretch shifts as the moisture content is varied. The sample used for measuring the visible Raman spectra of

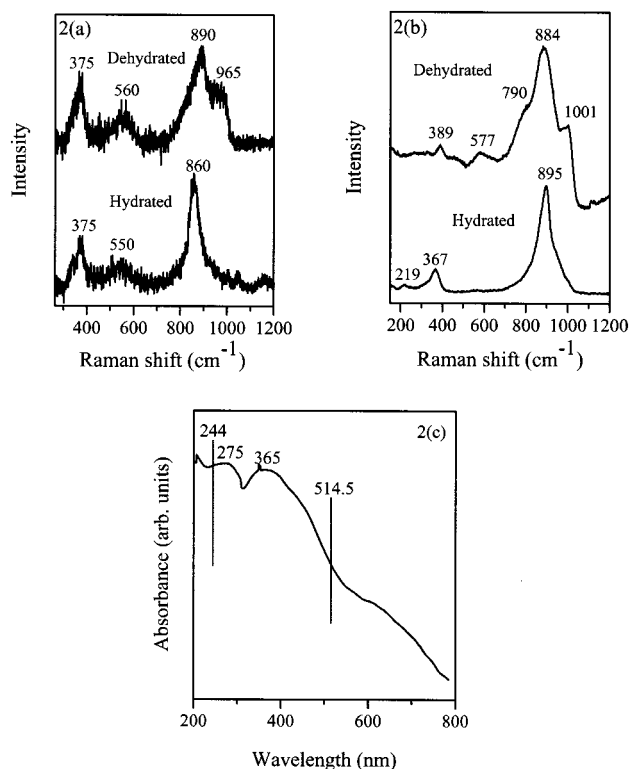


Figure 2. (a) UV Raman spectra of hydrated and dehydrated 5% $\text{CrO}_3/\text{Al}_2\text{O}_3$. (b) Visible Raman spectra of hydrated and dehydrated 5% $\text{CrO}_3/\text{Al}_2\text{O}_3$. (c) UV–visible diffuse reflectance spectra of hydrated 5% $\text{CrO}_3/\text{Al}_2\text{O}_3$.

the dehydrated 0.5% $\text{CrO}_3/\text{Al}_2\text{O}_3$ has a negligible water content since the spectrum was recorded after calcination, under controlled atmosphere conditions. The water content in the corresponding UV Raman spectrum is likely to be higher since the measurement was performed under ambient conditions and the dehydration produced by laser-induced heating may not be complete.

1b. 5% $\text{CrO}_3/\text{Al}_2\text{O}_3$ ($\sim 40\%$ monolayer). The UV and visible Raman spectra of 5% $\text{CrO}_3/\text{Al}_2\text{O}_3$ are shown in Figure 2, parts a and b. For the UV Raman spectrum, the hydrated sample was recorded using the spiral procedure. The Raman bands at ~ 375 and 860 cm^{-1} correspond to the bending modes and symmetric stretch of the hydrated CrO_4^{2-} species, respectively. The shift of the symmetric stretch of hydrated CrO_4^{2-} from 846 to 860 cm^{-1} suggests that the sample is partially dehydrated. In addition, the broad band at $\sim 550\text{ cm}^{-1}$ (symmetric stretch of Cr–O–Cr) suggests the presence of a dimeric $\text{Cr}_2\text{O}_7^{2-}$ species in this sample.²⁴ The symmetric stretch of the dimeric species appears as a shoulder at the high wavenumber side of the 860 cm^{-1} band. For the corresponding visible Raman spectrum, the hydrated sample was measured using a spinning disk. The Raman bands at 219 cm^{-1} (bending mode of Cr–O–Cr), 367 cm^{-1} (bending modes of CrO_3 groups) and 895 cm^{-1} (symmetric stretch of CrO_3 groups) indicate the presence of the hydrated $\text{Cr}_2\text{O}_7^{2-}$ species. The symmetric stretch of CrO_4^{2-} (a shoulder at $\sim 860\text{--}870\text{ cm}^{-1}$) is relatively weaker than the symmetric stretch of CrO_3 groups (895 cm^{-1}) of the dimeric species.

On the basis of the relative Raman band intensities in the UV and visible Raman spectra, one might be tempted to draw conclusions concerning the relative abundance of monomeric and dimeric species on the sample. Conflicting conclusions would be made from the UV and visible Raman spectra. The UV and visible Raman spectra would suggest that hydrated CrO_4^{2-} and $\text{Cr}_2\text{O}_7^{2-}$ are the dominant species, respectively.

From this example, we see that it is not trivial to determine the relative abundances of the chemical species on a particular sample based solely on the relative band intensities because the Raman cross-sections of the various bands are not known. In addition, as the sample absorbs 244 nm photons (Figure 2c), there is the possibility of resonance enhancement under UV excitation which complicates the situation even further. (The absorption bands at ~ 275 nm and ~ 365 nm are due to a charge-transfer transition from oxygen ligands to chromium atoms in both hydrated CrO_4^{2-} and $\text{Cr}_2\text{O}_7^{2-}$.³¹) However, one can still monitor the changes in the relative abundance of different chemical species as a function of weight percent loadings of the supported metal oxide by comparing their relative Raman band intensity in the respective UV or visible Raman spectra. Following this argument, we can safely conclude that the percentage of dimeric species in the 5% $\text{CrO}_3/\text{Al}_2\text{O}_3$ is greater than in the 0.5% $\text{CrO}_3/\text{Al}_2\text{O}_3$ sample.

The UV and visible Raman spectra of the dehydrated sample were recorded using stationary samples (Figure 2, parts a and b) under ambient and controlled atmosphere conditions, respectively. The Raman bands at $389/375$ cm^{-1} (bending modes of CrO_3 terminal and CrO_2 bridging groups), $\sim 577/\sim 560$ cm^{-1} (symmetric stretch of bridging $\text{Cr}-\text{O}-\text{Cr}$), ~ 790 cm^{-1} (asymmetric stretch of bridging $\text{Cr}-\text{O}-\text{Cr}$), $884/890$ cm^{-1} (symmetric stretch of CrO_2), ~ 965 cm^{-1} (stretch of terminal CrO_3), and 1001 cm^{-1} (symmetric stretch of CrO_2) suggest the existence of polymeric species on the dehydrated samples.³⁰ We note that the Raman bands due to the bending modes of CrO_3 and CrO_2 groups and the symmetric stretch of $\text{Cr}-\text{O}-\text{Cr}$ groups do not appear at the same Raman shifts under UV and visible excitation. A possible reason is because of the different extents of dehydration in the samples as discussed in Section 1a.

The relative band intensities in the UV and visible Raman spectra of the dehydrated samples are different. The 375 cm^{-1} and ~ 560 cm^{-1} bands are relatively more pronounced under UV excitation; the ~ 790 cm^{-1} band is relatively weaker, and the 1001 cm^{-1} band is barely detected in the UV Raman spectrum. We suggest that these relative peak intensity variations in the two spectra may be due to different extents of resonance enhancement under UV irradiation. A lesser extent of sample dehydration for UV Raman spectra might also shift the ~ 790 and 1001 cm^{-1} bands so that they merge with the strong Raman bands at ~ 890 cm^{-1} and ~ 965 cm^{-1} and thus are barely detectable.

2. 20% $\text{V}_2\text{O}_5/\text{Al}_2\text{O}_3$ (~ 1 monolayer). The UV and visible Raman spectra of the hydrated and dehydrated 20% $\text{V}_2\text{O}_5/\text{Al}_2\text{O}_3$ are presented in Figure 3, parts a and b, respectively. For the hydrated samples, both UV and visible Raman spectra were recorded using spinning disks. When spinning disks were used, no dark circles were formed under the laser beam. Since polymers are dark in color, the absence of dark circles suggests that little or no polymeric compounds were produced due to surface dehydration. In addition, the UV Raman spectrum measured using the spiral procedure looks identical to the spectrum measured using spinning alone. Spectra measured at the two excitation wavelengths are significantly different. In the visible Raman spectrum there is a broad background, and the Raman bands are generally broad and overlap one another in certain regions of the spectrum. The differences in UV and visible Raman spectra are likely due to changes in the intensity pattern produced by resonance enhancement in the ultraviolet excited spectra. In support of this possibility we have compared UV and visible Raman spectra of the aqueous decavanadate

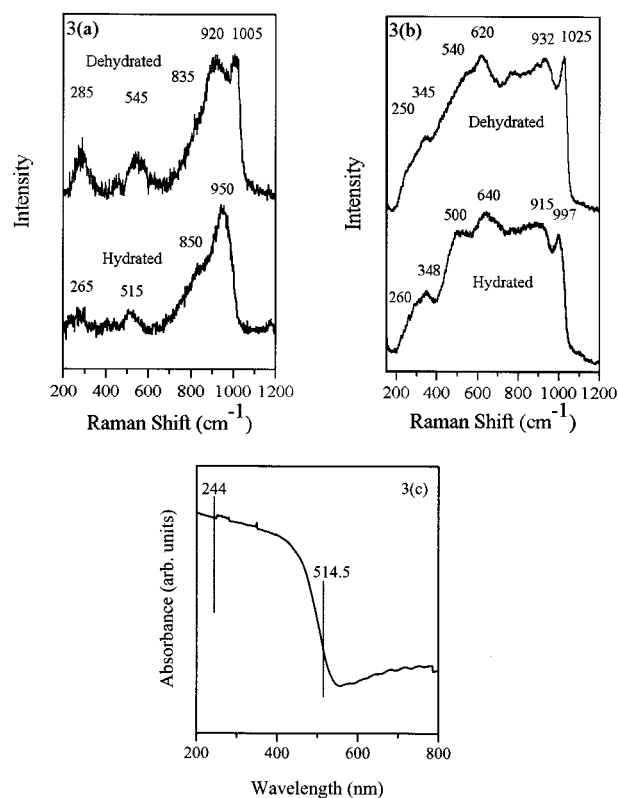


Figure 3. (a) UV Raman spectra of hydrated and dehydrated 20% $\text{V}_2\text{O}_5/\text{Al}_2\text{O}_3$ (monolayer). (b) Visible Raman spectra of hydrated and dehydrated 20% $\text{V}_2\text{O}_5/\text{Al}_2\text{O}_3$ (monolayer). (c) UV-visible diffuse reflectance spectra of hydrated 20% $\text{V}_2\text{O}_5/\text{Al}_2\text{O}_3$ (monolayer).

ion, $\text{V}_{10}\text{O}_{28}^{6-}$, and find that the Raman spectral intensity patterns are, indeed, very different for UV and visible excitation. (The Raman bands below 400 cm^{-1} correspond to the bending modes of $\text{V}-\text{O}-\text{V}$ groups. The symmetric and asymmetric stretching modes of the bridging $\text{V}-\text{O}-\text{V}$ groups are between ~ 450 cm^{-1} and ~ 850 cm^{-1} . The $\text{V}=\text{O}$ stretches are above 850 cm^{-1} .²⁵)

The UV and visible Raman spectra of the hydrated samples are also different in the following respects. The 348 and 640 cm^{-1} bands are only detected in the visible Raman spectra. The UV-visible diffuse reflectance spectra of this sample (Figure 3c) shows that the sample absorbs 244 nm radiation. A charge-transfer transition between the oxygen ligands and the vanadium metal centers occurs at ~ 220 nm.³² We suggest that these two bands are not detected because of relatively weaker resonance enhancements under UV excitation. In addition, the different peak positions of the $\text{V}=\text{O}$ stretch in the UV and visible Raman spectra is due to the presence of three types of $\text{V}=\text{O}$ stretches (~ 915 , 950 , and 997 cm^{-1}) and the $\text{V}=\text{O}$ stretch at 950 cm^{-1} is relatively more resonance enhanced than the other two bands under UV irradiation. It may also be due to the different degrees of hydration in the two samples as proposed in Section 1a, which causes bands to shift to higher or lower wavenumbers.

The UV and visible Raman spectra (Figure 3, parts a and b) of dehydrated 20% $\text{V}_2\text{O}_5/\text{Al}_2\text{O}_3$ indicate the presence of polymeric and mono-oxo vanadia species. The Raman bands of the polymeric species are at ~ 250 – 345 cm^{-1} ($\text{V}-\text{O}-\text{V}$ bend), ~ 540 – 620 cm^{-1} ($\text{V}-\text{O}-\text{V}$ symmetric stretch), ~ 835 cm^{-1} ($\text{V}-\text{O}-\text{V}$ asymmetric stretch), and $920/932$ cm^{-1} (OVO stretch).³⁰ In the UV Raman spectrum, the 345 and 620 cm^{-1} bands are not detected. Again this may be a result of the different resonance enhancement factors for different Raman bands. Among the vibrational modes, the vibrations at 345 and 620

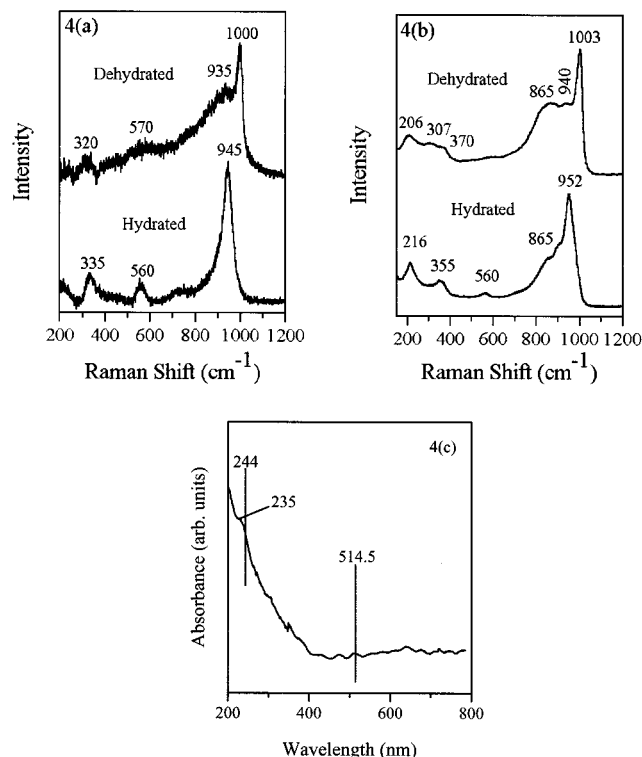


Figure 4. (a) UV Raman spectra of hydrated and dehydrated 18% MoO₃/Al₂O₃ (monolayer). (b) Visible Raman spectra of hydrated and dehydrated 18% MoO₃/Al₂O₃ (monolayer).

cm⁻¹ have the smallest resonance enhancements. The 1005 cm⁻¹ (UV Raman spectrum) and 1025 cm⁻¹ (visible Raman spectrum) bands are attributed to terminal V=O stretches from surface vanadia mono-oxo species.^{6,30} The difference in Raman shift of these two peaks could be due to two types of monooxo species, and the species with a V=O stretch at lower Raman shift is preferentially resonance enhanced under UV excitation. However, we believe that the explanation is more likely different degrees of dehydration in the two samples as proposed in Section 1a.

3. 18% MoO₃/Al₂O₃ (~1 monolayer). The UV and visible Raman spectra of the supported molybdenum oxides are presented in Figure 4, parts a and b, respectively. The UV and visible Raman spectra of the hydrated samples were measured using spinning disks. The Raman bands in the spectra are characteristic of hydrated heptamolybdate species, Mo₇O₂₄⁶⁻.²⁷ The Raman band of the Mo=O stretch appears at 945 cm⁻¹ in the UV Raman spectrum and 952 cm⁻¹ in the visible Raman spectrum. The Raman band of the Mo–O–Mo bending modes appears at 335 cm⁻¹ in the UV Raman spectrum and at 210 and 355 cm⁻¹ in the visible Raman spectrum. This sample absorbs 244 nm radiation (Figure 4c). The absorption band at ~235 nm is due to charge transfer from oxygen to the metal cations.³³ Furthermore, the 560 cm⁻¹ band (Mo–O–Mo symmetric stretch) is significantly stronger in the UV Raman spectrum, and the 865 cm⁻¹ band is more prominent in the visible Raman spectrum. Again these spectral variations may be due to the extent of resonance enhancement of different bands under UV excitation. These spectra may be compared to the results of Can Li and co-workers from a hydrated MoO₃/Al₂O₃ sample at much lower molybdenum loading (0.1%).³⁴ Their spectrum excited at 244 nm is similar to Figure 4a but without the band at 560 cm⁻¹. The absence of this band (Mo–O–Mo symmetric stretch) suggests that polymeric molybdate species are not present at the low loadings used in their study.

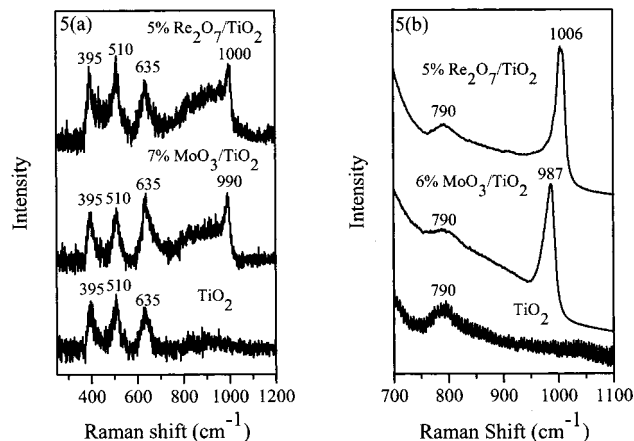


Figure 5. (a) UV Raman spectra of TiO₂ (anatase), dehydrated 7% MoO₃/TiO₂ (monolayer), dehydrated 5% Re₂O₇/TiO₂. (b) Visible Raman spectra of TiO₂ (anatase), dehydrated 6% MoO₃/TiO₂ (monolayer), dehydrated 5% Re₂O₇/TiO₂.

The UV and visible Raman spectra of dehydrated samples recorded with stationary disks are similar. The band at 1000/1003 cm⁻¹, assigned to a terminal Mo=O stretch, indicates the presence of a surface mono-oxo species.^{6,30} The other Raman bands in the spectra suggest the presence of a surface polymeric molybdenum oxide species.³⁰ The Raman bands from Mo–O–Mo bending vibrations of these surface polymeric species are below 400 cm⁻¹. The Raman bands of Mo–O–Mo symmetric and asymmetric stretches are between ~500 cm⁻¹ and ~900 cm⁻¹ while the OMoO symmetric stretch is at ~935/940 cm⁻¹.³⁰ The difference in relative intensities of the Raman bands due to the symmetric and asymmetric stretches of Mo–O–Mo groups in the two spectra may be attributed to different extents of resonance enhancement under UV excitation. As for the bending vibrations of Mo–O–Mo, their respective Raman band positions are the same in the visible and UV spectra within experimental error.

B. Titania-Supported Metal Oxides: 6–7% MoO₃/TiO₂ (~1 monolayer); 5% Re₂O₇/TiO₂ (~50% monolayer). Figure 5, parts a and b, show the UV and visible Raman spectra of the dehydrated TiO₂ support (Degussa P25), 6–7% MoO₃/TiO₂ and 5% Re₂O₇/TiO₂. The ultraviolet Raman bands at 395, 510, and 635 cm⁻¹ are associated with the fundamental vibrations of TiO₂ (anatase). The weak band at ~790 cm⁻¹ is assigned to the first overtone of the TiO₂ (anatase) 395 cm⁻¹ band. For the two supported metal oxides, the Raman bands at ~990 cm⁻¹ and ~1000 cm⁻¹ are due to surface mono-oxo species that are typically present under dehydrated conditions.⁶

In the visible Raman spectra of the titania-supported samples, the TiO₂ support bands are relatively much more intense than the bands of the surface metal oxide species. In fact the optical skin depth of TiO₂ is ~200 Å for 250 nm radiation and >40000 Å for 520 nm photons.³⁵ Under visible radiation, the volume of bulk TiO₂ sampled by the laser beam is much greater than under UV radiation. Hence, the ratio of the TiO₂ band intensity to the intensity of the surface metal oxides is much greater in the visible Raman spectra than in the UV Raman spectra. In Figure 5a, the band intensity of the stretching modes of the supported metal oxides (>700 cm⁻¹) are comparable to that of TiO₂. However, the bending and some M–O–M (M–Mo or M–Re) stretching vibrations that appear below 600 cm⁻¹ are still masked by the TiO₂ support bands.

C. General Comments about the UV and Visible Raman Spectra of Supported Metal Oxides. From these comparative studies of the same samples, some general comments can be

made concerning the UV and visible Raman spectra of supported metal oxides. In general, the spectra measured at the two wavelengths are remarkably similar in terms of the vibrational bands observed, their Raman shift, and their pattern of intensities. The most significant differences in the spectra are an apparent enhancement of the intensity of bands associated with the out-of-plane bending and symmetric stretching vibrations of bridging oxygen species (M–O–M) in the ultraviolet (e.g., see Figures 1, 2, and 4), and a corresponding enhancement of the intensity of bands associated with stretching vibrations of terminal metal–oxygen bonds (M–O and M=O) (see Figures 1, 2, and 3). We attribute these differences to resonance enhancement of the Raman scattering cross section under UV excitation.

Resonance enhancement is normally desirable as it increases detection sensitivity. Enhancements as large as 10^6 have been reported for molecular systems. However, for catalytic systems the question arises whether a measured spectrum could exhibit resonance Raman scattering effects to an extent that, for example, identification of the scattering species is no longer possible. Depending on the system under study, it is also possible for the resonance Raman scattering to be largely quenched due to a short lifetime for the electronically excited state. For example, the so-called A-term resonance Raman scattering³⁶ is given by:

$$A = \frac{1}{hc} [\mu_{\rho}^0]_{ge} [\mu_{\sigma}^0]_{eg} \sum_v \frac{\langle n_g | \nu_e \rangle \langle \nu_e | m_g \rangle}{\tilde{\nu}_{ev, gm} - \tilde{\nu}_0 + i\Gamma_{ev}} \quad (1)$$

The term $i\Gamma_{ev}$ in the denominator is the natural line width for the electronic excitation which is inversely related to the excited-state lifetime. For adsorbed species the excited state lifetime could be quite short due to strong coupling with the solid, leading to a value for the denominator that is comparable to the value for normal Raman scattering. This produces a resonance Raman spectrum that is similar to the normal Raman spectrum. While the out-of-plane bending and symmetric stretching modes of bridging oxygens appear to be resonantly enhanced, the enhancement is modest, and the UV excited spectra are quite similar to the visible excited spectra.

A negative consequence of absorption by solid samples in the ultraviolet is that fewer scatterers are sampled by the laser beam. The Raman band intensity of an absorbing sample is, therefore, a balance between the extent of resonance enhancement and the number of supported metal oxide species excited by the laser. As can be seen from the absorption measurements shown in Figures 2–4, the samples measured in this study are transparent or weakly absorbing in the visible and strongly absorbing in the ultraviolet. The signal-to-noise ratio in the visible Raman spectra are clearly higher than in the UV Raman spectra for the samples in this study. The extent of resonance enhancement for these samples is not sufficient to overcome the effect of the reduced number of scatterers. For catalysts that absorb strongly in both the visible and ultraviolet wavelength regions the number of scatterers contributing to the Raman spectrum will be comparable for the two wavelengths. Under these circumstances signal intensities in UV Raman measurements should be larger due to the larger scattering cross section.

The position of Raman bands associated with terminal oxygen stretching vibrations appear to be very sensitive to the degree of sample hydration. This is particularly evident in Figure 1 where the 855 cm^{-1} band measured under spiral conditions shifts to 873 cm^{-1} when only pure spinning is used to avoid laser-induced heating. This sensitivity certainly emphasizes the point

that careful attention to sample treatment during Raman measurements is essential for obtaining consistent, interpretable spectra. Under circumstances where a sample is strongly absorbing and dehydration is particularly severe, it may be advisable to use a fluidized bed technique to minimize laser-induced heating.³⁷

Conclusion

The Raman spectra of supported oxides excited by visible and ultraviolet wavelengths exhibit identical band positions within experimental error. The out-of-plane bending and symmetric stretching vibrations of bridging oxygen species are modestly resonance enhanced using ultraviolet excitation, but not to a degree that makes the spectrum unrecognizable compared to visible excitation. Thus, we conclude that the large body of Raman spectra from catalysts measured using visible lasers should be very useful for interpreting new measurements using ultraviolet lasers. For catalyst samples that are transparent in the visible and where interference from fluorescence is not a problem, the much larger signal intensities favors the use of visible excitation over ultraviolet excitation. When fluorescence interference is unavoidable, such as under catalytic conditions where carbon lay down occurs or when one of the catalyst components fluoresces strongly or when the catalyst absorbs strongly in both visible and ultraviolet wavelength regimes, ultraviolet excitation is favored. Under any circumstances special care must be exercised to avoid laser-induced artifacts arising from heating or photochemistry.

Acknowledgment. Financial support of this work was provided by the Department of Energy, Office of Basic Energy Sciences, Division of Chemical Sciences, under Contracts DE-FG02-97ER14789 (Northwestern) and DE-FG02-93ER14350 (Lehigh).

References and Notes

- (1) Wachs, I. E.; Segawa, K. In *Characterization of Catalytic Materials*; Wachs, I. E., Ed.; Butterworth-Heinemann: Boston, 1992; Chapter 4.
- (2) Turek, A. M.; Wachs, I. E.; Decanio, E. J. *Phys. Chem.* **1992**, *96*, 5000.
- (3) Segawa, K.; Hall, W. K. *J. Catal.* **1982**, *76*, 133.
- (4) Segawa, K.; Hall, W. K. *J. Catal.* **1982**, *77*, 221.
- (5) Busca, G.; Lavalley, J. C. *Spectrochim. Acta* **1986**, *42A*, 443.
- (6) Wachs, I. E. *Catal. Today* **1996**, *27*, 437.
- (7) Stencel, J. M. *Raman Spectroscopy for Catalysis*; van Nostrand Reinhold: New York, 1990.
- (8) Mehicic, M.; Grasselli, J. G. In *Analytical Raman Spectroscopy*; Grasselli, J. G., Bulkin, B. J., Eds.; John Wiley & Sons: New York, 1991; Chapter 10.
- (9) Ortins, N. J.; Kruger, T. A.; Dutta, P. K. In *Analytical Applications of Raman Spectroscopy*; Pelletier, M. J., Ed.; Blackwell Science: Oxford, 1999; Chapter 8.
- (10) Weckhuysen, B. M.; Wachs, I. E. *J. Phys. Chem.* **1996**, *100*, 14437.
- (11) Went, G. T.; Leu, L.-J.; Rosin, R. R.; Bell, A. T. *J. Catal.* **1992**, *134*, 492.
- (12) Wang, C. B.; Cai, Y. P.; Wachs, I. E. *Langmuir* **1999**, *15*, 1223.
- (13) Dutta, P. K.; Zaykoski, R. E. *Zeolites* **1988**, *8*, 179.
- (14) Jeziorowski, H.; Knozinger, H. *Chem. Phys. Lett.* **1977**, *51*, 519.
- (15) Hendra, P.; Jones, C.; Warnes, G. *Fourier Transform Raman Spectroscopy: Instrumentation and Chemical Applications*; Ellis Horwood: New York, 1991; pp 246–258.
- (16) Asher, S. A.; Johnson, C. R. *Science* **1984**, *225*, 311.
- (17) Li, C.; Stair, P. C. In *Progress in Zeolite and Microporous Materials*; Stud. Surf. Sci. Catal.; Chon, H., Ihm, S.-K., Uh, Y. S., Eds.; Elsevier: Amsterdam, 1997; Vol. 105, p 599.
- (18) Li, C.; Stair, P. C. In *11th International Congress on Catalysis—40th Anniversary*; Stud. Surf. Sci. Catal.; Hightower, J. W., Delgass, W. N., Iglesia, E., Bell, A. T., Eds.; Elsevier: Amsterdam, 1996; Vol. 101, p 881.
- (19) Li, C.; Stair, P. C. *Catal. Lett.* **1996**, *36*, 119.
- (20) Li, C.; Stair, P. C. *Catal. Today* **1997**, *33*, 353.
- (21) Stair, P. C.; Li, C. *J. Vac. Sci. Technol.* **1997**, *A15*, 1679.

- (22) Li, C.; Xiong, G.; Xin, Q.; Liu, J. K.; Ying, P. L.; Feng, Z. C.; Li, J.; Yang, W. B.; Wang, Y. Z.; Wang, G. R.; Liu, X. Y.; Lin, M.; Wang, X. Q.; Min, E. Z. *Angew. Chem., Int. Ed.* **1999**, *38*, 1999.
- (23) Liu, S. L.; Xiong, G. X.; Yang, W. S.; Xu, L. Y.; Xiong, G.; Li, C. *Catal. Lett.* **1999**, *63*, 167.
- (24) Hardcastle, F. D.; Wachs, I. E. *J. Mol. Catal.* **1988**, *46*, 173.
- (25) Deo, G.; Wachs, I. E. *J. Phys. Chem.* **1991**, *95*, 5889.
- (26) Deo, G.; Hardcastle, F. D.; Richards, M.; Wachs, I. E.; Hirt, A. M. In *Novel Materials in Heterogeneous Catalysis*; Baker, R. T. K., Murrell, L. L., Eds.; ACS Symposium Series 437; American Chemical Society: Washington, DC, 1990; p 317.
- (27) Kim, D. S.; Segawa, K.; Soeya, T.; Wachs, I. E. *J. Catal.* **1992**, *136*, 539.
- (28) Vuurman, M. A.; Stufkens, D. J.; Oskam, A.; Wachs, I. E. *J. Mol. Catal.* **1992**, *76*, 263.
- (29) Michel, G.; Machiroux, R. *J. Raman Spectrosc.* **1983**, *14*, 23.
- (30) Vuurman, M. A.; Wachs, I. E. *J. Phys. Chem.* **1992**, *96*, 5008.
- (31) Radhakrishna, S.; Sharma, B. D. *J. Chem. Phys.* **1974**, *61*, 3925.
- (32) Tadros, Th. F.; Sadek, H.; El-Harakani, A. A. *Z. Phys. Chem. (Leipzig)* **1969**, *242*, 1.
- (33) Malik, A.; Zubairi, S. A.; Khan, A. S. *J. Chem. Soc., Dalton Trans.* **1977**, 1049.
- (34) Xiong, G.; Li, C.; Feng, Z.; Ying, P.; Xin, Q.; Liu, J. *J. Catal.* **1999**, *186*, 234.
- (35) The value of the optical skin depth, d , is calculated from the equation $d = \lambda/2\pi k$, where λ is the wavelength of the excitation source and k is the extinction coefficient obtained from the following references. (a) Joseph, J.; Gagnaire, A. *Thin Solid Films* **1983**, *103*, 257. (b) *Handbook of Optical Constants of Solids*; Palik, E. D., Ed.; Academic Press: New York, 1985; p 795.
- (36) Clark, R. J. H.; Dines, T. J. *Angew. Chem.* **1986**, *98*, 131.
- (37) Chua, Y. T.; Stair, P. C. *J. Catal.* **2000**, *196*, 66.